

Enhanced UV Emission in Silicon Nanoparticles

Akhilesh K. Singh, Karol G. Grycznski, Jianyou Li, F. McDaniel, B. Rout, and Arup Neogi
Department of Physics, University of North Texas, Denton, TX, USA.

Gayatri Sahu, Haraprasanna Lenka, Durga P. Mahapatra
Institute of Physics, Orissa, India

ABSTRACT

Direct bandgap emission was observed from quantum confined Silicon nanoparticles synthesized by a novel dual-ion beam implantation technique. Quantum dots (QDs) were formed due to recrystallization of silicon in the amorphous layer due to the irradiation of high energy ions (~MeV). Structural analysis such as High Resolution Transmission Electron Microscopy (HRTEM) and X-ray confirm the formation of silicon QDs. FTIR absorption spectroscopy was performed to analyze the formation of silicon quantum dots due to annealing of the ion-implanted samples. Strong room-temperature emission (with FWHM ~ 87 meV) was observed from the Si quantum dots which splits into multiple lines at lower temperature. The splitting of PL peak observed at lower temperature has been analyzed using the effective mass approximation

Keywords: Quantum Dots (QDs), Photoluminescence (PL), Optoelectronics, Ion Implantation, Silicon Photonics.

1 Introduction

As optoelectronic devices move towards commercial viability it is necessary to engineer materials with suitable electrical and optical properties to be used in such devices. The necessity of moving these materials from an academic developmental setting to industrialization and mass production is also an important consideration. Silicon based optoelectronic devices offer many advantages over existing III-V semiconductor materials to achieve monolithically integrated optoelectronic circuit with higher packing densities and lower energy requirements¹. This translates directly into smaller/thinner device which are less expensive to operate. Breakthroughs in Si as an optoelectronic material may lead to inexpensive optical transceivers, modulators, waveguides and detectors.

However the use of Silicon as an optoelectronic material is hampered due to its indirect band gap in bulk form. Recently the synthesis of silicon nanocrystal is has opened up the feasibility of its use in optoelectronics. In nanoscale sizes silicon can emit light from quantum dots (QDs), dangling bonds, and by forming silicides with metals such as gold². Silicon based nanostructures can be readily integrated with existing manufacturing processes and is relatively inexpensive. QDs in silicon can be created in silicon or silicon oxides through various techniques

including chemical etching, chemical vapor deposition (CVD), and ion implantation. These methods can result in luminescence anywhere from the infra red (IR) to ultraviolet (UV), depending on the size of the quantum dots due to quantum confinement³. However there are no prior reports on the direct bandgap emission from the quantum dots as the lifetime of the emission is dictated by intervalley scattering leading to microsecond decay feature. The competing Auger recombination and other nonradiative processes reduces the internal quantum efficiency of the Si nanostructures

In this paper, a method for fabrication of optically active silicon with direct bandgap emission is presented and ways to enhance the system's efficiency are discussed. Quantum dot (QD) formation in an undoped silicon wafer was induced using multiple ion beam implantation which facilitates recrystallization in the Si system. Structural and optical characterization was performed and comparisons of growth parameters were analyzed.

2 Sample Synthesis

Sample preparation involves sequential ion beam treatment and oven annealing of a crystalline silicon wafer (c-Si) instead of conventional SiO_x layers. The Si(100) wafers are undoped and untreated except for the removal of the oxide layer before ion-implantation. First the sample is treated with a lower energy beam in the order of a few dozen keV. This beam leads to the creation of an amorphous silicon (α -Si) layer with nanocrystalline silicon structures formed within the layers exposed to the ion beam radiation. Second the wafer is treated with the annealing beam with energy on the order of a few MeV. The ions from this treatment penetrate far beyond the α -Si region and play a significant role in modifying the surface of silicon nanocrystals formed in the first stage. These high energy ions deposit large amounts of energy due to electronic interactions within α -Si layer and crystalline silicon nanostructure. This energy is believed to anneal the surface of the crystalline nanostructures and passivate the dangling bonds, which normally act as dominant non-radiative recombination centers. Finally the samples are oven annealed in a quartz tube furnace at 500 °C for one hour, which is expected to migrate the quantum dots close to the sample surface. The migration of the nanoparticles towards the surface is expected to reduce the reabsorption of light emission from the nanoparticles by the Si matrix.

3 Experiment and Discussion

The samples were synthesized using the technique outlined in Reference 4. The reference sample was a Si(100) substrate treated with a single species ion beam. Implantation on this sample was done using a silicon ion source at 45 keV with a fluence of 10^{15} atoms / cm^2 . The other samples were prepared by sequential gold ion beam treatments. First the samples were treated with an annealing beam with energy of 32 keV. Second the samples were treated with an annealing beam with energy of 3 MeV. Finally one of the gold samples was annealed in a quartz tube furnace at 500 °C for one hour⁴.

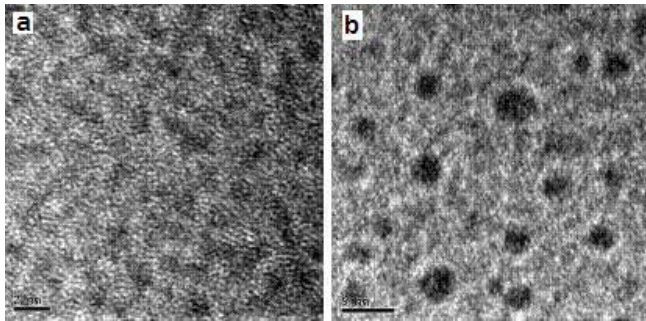


Figure 1 HRTEM images of Si QDs prepared by (a) silicon and (b) gold ion treatment.

It is observed that the quantum dots are formed even with low energy beam implantation. However, the annealing beam is responsible for recrystallization process and possibly the passivation of QD surface as observed in Figure 1. Fig 1a shows a HRTEM image of the Si prepared sample, for which only the annealing (keV) beam was used. Nanoparticles with an average size of two nanometers are clearly visible. Fig 1b shows a HRTEM micrograph of the gold treated annealed sample, the particle size also averages to two nanometers. It should be noted that nanoparticles of similar dimension are produced with both Si and Au ions. From a statistical analysis of the TEM spectrum we observe that almost 20% of the quantum dots have a diameter of 2nm

Cross sectional HR-TEM is used to determine the depth of the α -Si layer. Figure 2 shows such an image for the silicon treated sample, from this image it can be determined that the depth of the amorphous layer is ~110nm. In the micrograph c-Si is seen on the bottom and the α -Si layer is on top of it. The higher contrast in the gold treated sample is due to enhanced crystalline quality, which is confirmed by the narrow full-width at half maximum of the diffraction profile observed from the X-Ray Diffraction (XRD) measurements (Fig 3). Also the absence of the Si(311) peak in the spectra for the gold annealing sample indicates that the annealing beam by itself cannot remove it. This is most likely due to the local heating induced by the ion beam implantation process.

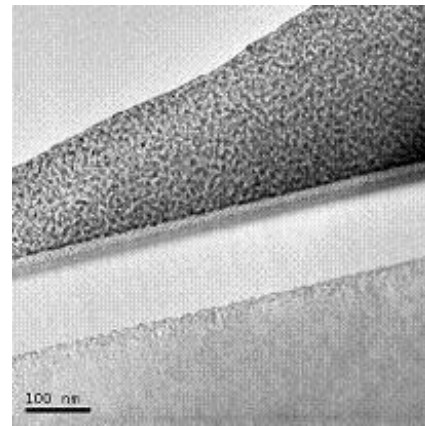


Figure 3 Cross Sectional HRTEM of silicon treated wafer.

Sample composition is analyzed using Fourier Transform Infrared Spectroscopy (FTIR). Figure 4 shows the FTIR transmission for the Au annealed sample and the Si treated sample. It should be noted that the gold implanted samples has several additional absorption peaks which are not observed in the silicon implanted samples. Si-Si and Si-O-Si bonds are present in both samples. The additional infrared absorption lines in the gold treated sample shows the modification of the original sample due to ion-implantation process induced by the modification of surface charges or dangling bonds. It does not appear to induce additional optical transitions in the UV-Visible optical spectrum except for the modification in the magnitude of the optical intensity. The additional bonds induced by the Au implantation are likely to modify the radiative efficiency and carrier confinement in the nanoparticles as observed from the enhancement in luminescence efficiency likely due to the modification of the oscillator strength.

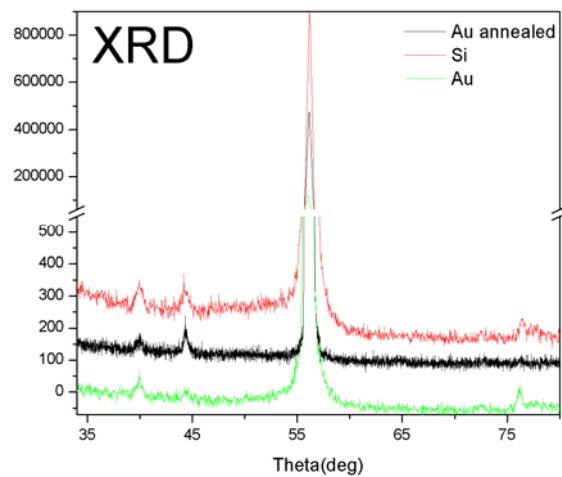


Figure 2 XRD spectra of silicon wafer treated with Si (red), gold (green), and gold with annealing (black)

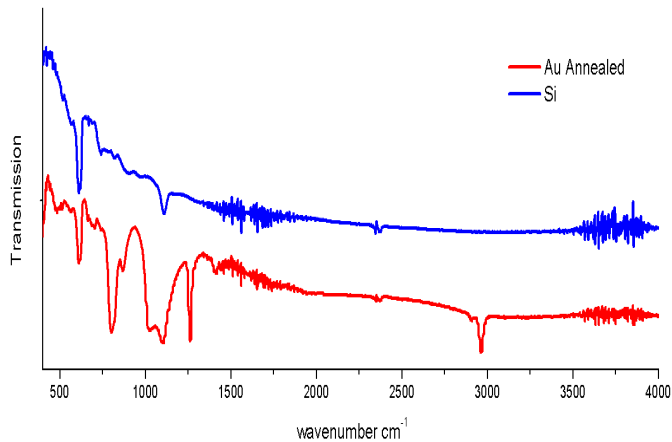


Figure 4 FTIR spectra of silicon wafer treated with silicon (blue) and gold (red) ions

Photoluminescence (PL) spectrum is measured using a He-Cd laser with an excitation wavelength of 325 nm (3.81 eV). Figure 5 shows temperature dependence PL spectra. At room temperature the sample luminesces with a peak emission at 3.3 eV. The FWHM at 300 K is 87 meV which is lower than previously reported values. It is observed that the emission spectrum splits into four different emission lines at low temperatures

The full FWH are the lowest reported for Si-QDs at both room and lower temperatures and comparable to III-V quantum dots. At room temperature the FWHM is 87 meV and at 77K temperature the narrowest peak has a width of 25 meV. Shifts in peak centers are negligible as the temperature varies, while the FWHM increases with

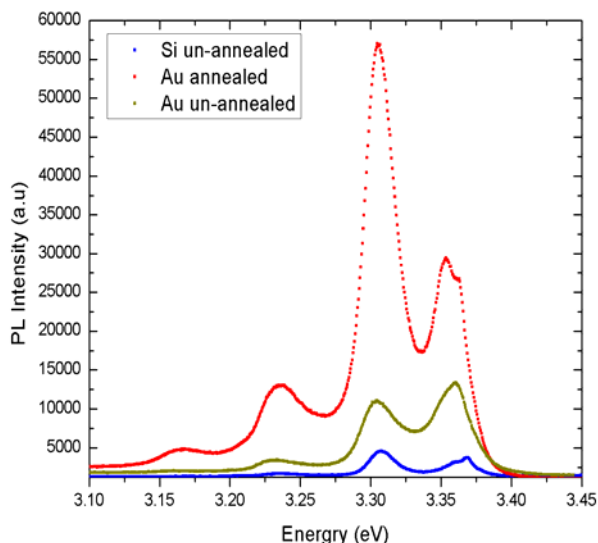


Figure 5 PL spectra at 77K for silicon wafers treated with silicon (blue), gold (yellow), and gold with annealing (red).

raising temperature as expected. The spacing between all pairs of the four prominent peaks is 47 meV, 63 meV, and 45 meV from left to right. In Figure 5, the PL spectrums were measured at 77K. It is observed that there is no additional optical transition induced by the Au beam implantation and is identical to the emission from the Silicon implanted samples. A comparison of Figure 1, 3 and Figure 5 shows that as the crystalline quality of the Si nanoparticles increases we observe a corresponding enhancement in the light emission. The splitting is similar to exciton splitting or the emission from the high energy states from crystalline Si nanoparticles. These emissions are not from quantum dots of various sizes as observed from the uniformity of emission from the sample surface.

Temperature dependent spectra (Fig. 6) reveal a slight blue shift as temperature decreases, roughly 0.01 eV as temperature varies from 77K to 300K. The FWHM increases with temperature while intensity decreases with increasing temperature due to phonon and other interfacial effects. We have observed UV light emission around 3.3 eV which at 77 k splits into four peak energies roughly at 3.19, 3.24, 3.30, 3.35 with 169, 44.3, 24.1 and 28.2 meV FWHM respectively.

When we consider an infinite potential barrier, the energy gap E for a Si QD confined in three dimensions can be expressed as $E(\text{eV}) = E_{\text{bulk}} + (C/d^2)$ according to effective mass theory, E is the bulk crystal silicon band gap, and C is the confinement parameter, and d is the QD size. Band gap energy was obtained from PL measurements, bulk energy of c-Si from literature and QD size from HRTEM images, the confinement parameter was calculated to be $8.56 \text{ eV} \cdot \text{nm}^2$. Using the above equation we can clearly see that our distinct energies at low temperature do not result from different size dots; no emission is visible at the expected energies for QDs with size difference of 0.1 nm. Calculations based on Effective mass theory show that QDs of 2.1 nm and 1.9 nm would produce transition energies of 3.10 eV and 3.53 eV respectively, which are not observed from the emission spectra. 8% of the nanoparticles are observed to be around these sizes, which are not optically active. We believe that different size dots are not active due to their low concentration or other recombination effects. The role of Au silicides in the emission has been ruled out as the emission from the nanostructures is observed even with Si implanted samples at low temperature without any Au implants. Time-resolved measurements (not presented here) shows sub-nanosecond carrier recombination rates a low temperature with high radiative efficiency which demonstrates the direct bandgap nature of the quantum dots formed by ion-beam implantation. The carrier recombination demonstrates a direct nature of the photoluminescence dominated by radiative process which will be presented in the talk.

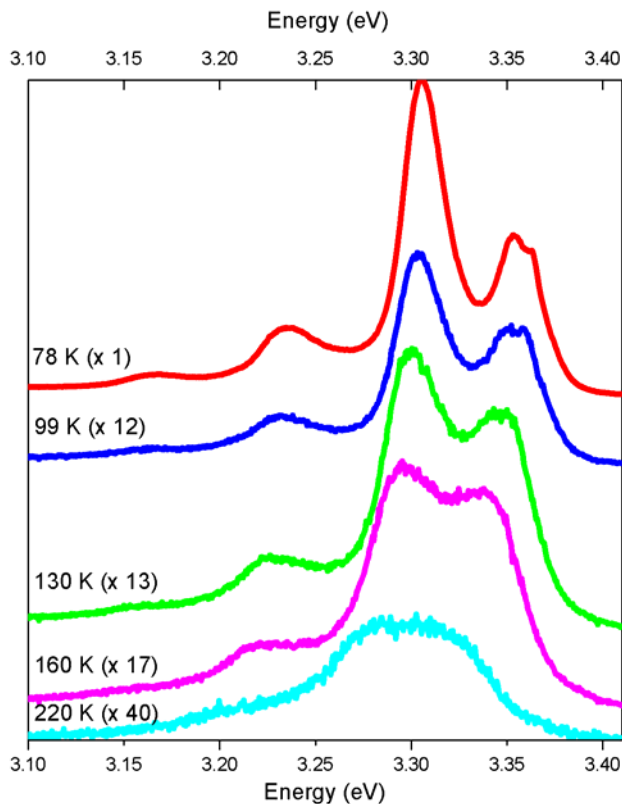


Figure 6 Temperature dependent PL for Si wafer treated with Au beam and annealed.

4 Conclusion

It is theorized that the peak splitting is caused by emission from different energy states of the 2 nm QDs. This agrees with room temperature PL that energy level of quantum dot is continuum i.e. UV emission peak at nearly 3.3 eV, providing a FWHM of 87 meV which is narrower than previous work⁵. Our observations agree with literature on two nm Si QDs using infinite barriers⁶. Thus, PL along with HRTEM measurement results verify the quantum confinement effect in silicon quantum dot system of ion beam treated silicon wafers. Using effective mass theory such splitting would require resolution of from QDs which differ by 0.022nm in diameter. Thus we disregard the possibility that this splitting is caused by QDs of different sizes.

It is thus theorized that this splitting is caused by the excitonic transitions from various distinct energy levels of the QDs. HRTEM images show that c-Si QDs are present within the a-Si matrix; the bandgap difference of such a system is 0.5 eV. The gold treated samples show an enhancement in PL intensity of almost two orders of magnitude over the reference silicon treated sample. The annealed sample is believed to have superior enhancement to the non annealed sample because of an increase in crystalline nature which results in a sharper boundary between the QDs and the amorphous matrix. This result

will offers interesting prospects for Silicon based optoelectronics and will be key for Silicon Photonics.

ACKNOWLEDGEMENT

This work was supported by NSF-IRES program and NSF-MRI program. We would like to acknowledge the invaluable contributions of Dr. David Diercks at the Center for Advanced Research and Technology (CART), University of North Texas for structural charecterization.

This work is supported in part by The National Science Foundation and The Welch Foundation.

REFERENCES

- ¹ G. Overton, Optoelectronic Worldnews, 42,28 (2006)
- ² U. Bockelmann and t. Egeler, Phys. Rev. B 46, 15574 (1992)
- ³ Tae-Youb Kim, Nae-Man Park, Kyung-Hyun Kim, Gun Yong Sung Young-Woo Ok, Tae-Yeon Seong and Cheol-Jong Choi, Appl.Phys. Lett. 85, 5355 (2004)
- ⁴ G. Sahu, B Joseph, H P Lenka, P K Kuri, A Pradhan and D P Mahapatra, Nanotechnology 18, 495702 (2007)
- ⁵ Katshuiro Tomioka and sadao Adachi, Appl.Phys. Lett. 87, 251920 (2005)
- ⁶ Nae-Man Park, Chel-Jong Choi, Tae-Yeon Seong, and Seong-Ju Park, Phys. Rev. Lett. 86, 1355(2001)